A-PRIORI DNS MODELLING OF CO-VARIANCE TRANSPORT IN TURBULENT STRATIFIED FLAMES

S.P. Malkeson[*] and N. Chakraborty[*]
n.chakraborty@liverpool.ac.uk
[*]School of Engineering, University of Liverpool
Liverpool, L69 3GH, United Kingdom

Abstract

Three-dimensional simplified chemistry based Direct Numerical Simulations (DNS) of statistically planar turbulent stratified flames at global equivalence ratios $<\phi>=0.7$ and $<\phi>=1.0$ have been carried out to analyse the statistical behaviour of the transport of co-variance of the fuel mass fraction Y_F and mixture fraction ξ fluctuations (i.e. $\overline{\rho Y_F'' \xi''}/\overline{\rho}$) for Reynolds Averaged Navier Stokes simulations where $\overline{q}$, $\tilde{q} = \overline{\rho q}/\overline{\rho}$ and $q'' = q - \tilde{q}$ are Reynolds averaged, Favre mean and Favre fluctuation of a general quantity q with ρ being the gas density and the overbar suggesting a Reynolds averaging operation. It has been found that existing algebraic expressions cannot adequately capture $\overline{\rho Y_F'' \xi''}/\overline{\rho}$ behaviour for low Damköhler number combustion and therefore, a transport equation for $\overline{\rho Y_F'' \xi''}/\overline{\rho}$ may need to be solved. The statistical behaviours of $\overline{\rho Y_F'' \xi''}/\overline{\rho}$ and the unclosed terms of its transport equation (i.e. the terms originating from turbulent transport T_1, reaction rate T_4 and molecular dissipation D_2) have been analysed in detail. Through an *a-priori* DNS analysis, the performances of the models for T_1, T_4 and D_2 have been assessed.

Introduction

In turbulent stratified flames, the co-variance of fuel mass fraction Y_F and mixture fraction ξ fluctuations is often required for reaction rate closure [1-3]. In the context of Reynolds Averaged Navier Stokes (RANS) simulations, the co-variance of Y_F and ξ fluctuations is given by $\overline{\rho Y_F'' \xi''}/\overline{\rho}$. Mura *et al.* [3] proposed an algebraic expression for $\overline{\rho Y_F'' \xi''}/\overline{\rho}$ for turbulent stratified flames. An *a-priori* DNS analysis by Malkeson and Chakraborty [4] demonstrated that the algebraic expression proposed by Mura *et al.* [3] may not adequately account for the statistical behaviour of $\overline{\rho Y_F'' \xi''}/\overline{\rho}$ for low Damköhler number *Da* combustion, and such cases may require the solving of a modelled transport equation of $\overline{\rho Y_F'' \xi''}/\overline{\rho}$. To date there has not been a study in the existing literature where the transport of $\overline{\rho Y_F'' \xi''}/\overline{\rho}$ is addressed and modelling of the unclosed terms are analysed based on an *a-priori* analysis of DNS data. Thus, it is useful to analyse the statistical behaviour of co-variance $\overline{\rho Y_F'' \xi''}/\overline{\rho}$ transport under low Damköhler number conditions to address this void in the existing literature. In this respect, the main objectives are as follows:

1. To analyse the statistical behaviour of the unclosed terms of the $\overline{\rho Y_F'' \xi''} / \overline{\rho}$ transport equation, especially under low Da conditions in the context of RANS simulations.
2. To identify appropriate models for the unclosed terms of the $\overline{\rho Y_F'' \xi''} / \overline{\rho}$ transport equation in the context of RANS by comparing the model predictions with the corresponding quantities extracted from DNS data.

The necessary mathematical background and the numerical implementation details will be presented briefly in the next section. Following this, the results will be presented and subsequently discussed. Finally, the main conclusions will be drawn.

Mathematical Background and Numerical Implementation

Ideally both three-dimensionality of turbulence and detailed chemical mechanism should be accounted for in combustion DNS studies, but such simulations still remain extremely expensive. For an extensive parametric study, three-dimensional DNS simulations have been carried out where a single-step irreversible Arrhenius-type chemical mechanism has been modified to mimic the realistic $S_{b(\phi)}$ variation with ϕ for hydro-carbon flames [5]. In this study, viscosity μ, thermal conductivity λ and density-weighted mass diffusivity ρD are taken to be equal for all species, and independent of temperature. The Lewis numbers $Le = \alpha_T / D$ of all species are taken to be unity. The species field in stratified flames is often characterised in terms of Y_F and ξ. The mixture fraction ξ is defined as:

$$\xi = (Y_F - Y_O / s + Y_{O\infty} / s) / (Y_{F\infty} + Y_{O\infty} / s) \quad (1)$$

where Y_O is the oxidiser mass fraction, $Y_{O\infty}$ is the oxidiser mass fraction in air and $Y_{F\infty}$ is the fuel mass fraction in the pure fuel stream. The values for s, $Y_{F\infty}$ and $Y_{O\infty}$ are taken to be $s = 4$; $Y_{F\infty} = 1.0$ and $Y_{O\infty} = 0.233$, which yields the stoichiometric fuel mass fraction (mixture fraction) $Y_{Fst} = 0.055$ ($\xi_{st} = 0.055$). These values are representative of methane-air combustion. For stratified flames, a reaction progress variable c can be defined in terms of Y_F, so that it rises monotonically from 0 (in unburned reactants) to 1 (in fully burned products) [4,6]:

$$c = (\xi Y_{F\infty} - Y_F) / [\xi Y_{F\infty} - \max[0, (\xi - \xi_{st}) / (1 - \xi_{st})] Y_{F\infty}] \quad (2)$$

Mura *et al*. [3] have proposed an algebraic expression for $\overline{\rho Y_F'' \xi''} / \overline{\rho}$ for turbulent stratified flames based on a presumed probability density function (pdf) approach, where combustion is assumed to take place in thin flamelets, and the Favre joint pdf $\widetilde{P}(Y_F, \xi)$ is modelled as:

$$\widetilde{P}(Y_F, \xi) = \rho P(Y_F, \xi) / \overline{\rho} = \lambda_W \widetilde{P}(\xi | Y_{\max}) \delta(Y_F - Y_{\max}(\xi)) + (1 - \lambda_W) \widetilde{P}(\xi | Y_{\min}) \delta(Y_F - Y_{\min}(\xi)) + O(1/Da) \quad (3)$$

where $P(\xi | Y_F)$ is the pdf of ξ conditional on Y_F and the quantities $Y_{\max}(\xi) = \xi$ and $Y_{\min}(\xi) = A(\xi)(\xi - \xi_{st})$ are maximum and minimum values of Y_F according to the Burke-Schumann diagram, where $A(\xi)$ is given by $A(\xi) = H(\xi - \xi_{st}) / (1 - \xi_{st})$ where $H(\xi - \xi_{st})$ is a Heaviside function [1-3]. For $Da >> 1$, the chemical time remains infinitely small for any value of ξ, and thus λ_W is unlikely to depend on ξ which leads to the condition: $\widetilde{P}(\xi | Y_{\max}) = \widetilde{P}(\xi | Y_{\min})$ [3]. Using eq. 3 in $\widetilde{Y}_F = \int Y_F \widetilde{P}(Y_F, \xi) dY_F d\xi$ yields:

$$\lambda_W = (\widetilde{Y}_F - \widetilde{Y}_{\min}) / (\widetilde{Y}_{\max} - \widetilde{Y}_{\min}) \quad (4)$$

Based on eq. 3, Mura *et al.* [3] derived the following algebraic expression for $\overline{\rho Y_F'' \xi''}/\overline{\rho}$:

$$\overline{\rho Y_F'' \xi''}/\overline{\rho} = [(\tilde{Y}_F - \tilde{Y}_{\min})/(\tilde{Y}_{\max} - \tilde{Y}_{\min}) + (\tilde{Y}_{\max} - \tilde{Y}_F)/(\tilde{Y}_{\max} - \tilde{Y}_{\min})\tilde{A}] \times \overline{\rho \xi''^2}/\overline{\rho} = [\lambda_W + (1-\lambda_W)\tilde{A}] \times \overline{\rho \xi''^2}/\overline{\rho} \quad (5)$$

For RANS simulations, the transport equation of $\overline{\rho Y_F'' \xi''}/\overline{\rho}$ takes the following form [2]:

$$\frac{\partial}{\partial t}\left(\overline{\rho} \tilde{Y_F'' \xi''}\right) + \frac{\partial}{\partial x_j}\left(\overline{\rho} \tilde{u}_j \tilde{Y_F'' \xi''}\right) = \underbrace{\frac{\partial}{\partial x_j}\left[\rho D \frac{\partial \tilde{Y_F'' \xi''}}{\partial x_j}\right]}_{D_1} \underbrace{- \frac{\partial(\overline{\rho u_j'' Y_F'' \xi''})}{\partial x_j}}_{T_1} \underbrace{- \overline{\rho u_j'' \xi''} \frac{\partial \tilde{Y}_F}{\partial x_j}}_{T_2} \underbrace{- \overline{\rho u_j'' Y_F''} \frac{\partial \tilde{\xi}}{\partial x_j}}_{T_3} + \underbrace{(\overline{\dot{\omega}_F \xi} - \overline{\dot{\omega}} \tilde{\xi})}_{T_4} \underbrace{- 2\overline{\rho} \tilde{\varepsilon}_{Y\xi}}_{D_2} \quad (6)$$

where u_j is the velocity component in the j^{th} direction, $\dot{\omega}_F$ is the reaction rate of fuel, D is the fuel mass diffusivity and $\tilde{\varepsilon}_{Y\xi} = \overline{\rho D \nabla Y_F'' \cdot \nabla \xi''}/\overline{\rho}$ is the cross-scalar dissipation rate. The first (second) term on the left hand side of eq. 6 denotes the transient (mean advection) effects on $\overline{\rho Y_F'' \xi''}/\overline{\rho}$ transport. The term D_1 signifies the molecular diffusion of $\overline{\rho Y_F'' \xi''}/\overline{\rho}$. The term T_1 denotes the turbulent transport of $\overline{\rho Y_F'' \xi''}/\overline{\rho}$, and the terms T_2 and T_3 indicate generation/destruction of $\overline{\rho Y_F'' \xi''}/\overline{\rho}$ by mean scalar gradients $\partial \tilde{Y}_F/\partial x_j$ and $\partial \tilde{\xi}/\partial x_j$ respectively. The term T_4 denotes the chemical reaction rate contribution to $\overline{\rho Y_F'' \xi''}/\overline{\rho}$ transport and $-D_2$ signifies the effects of molecular dissipation of $\overline{\rho Y_F'' \xi''}/\overline{\rho}$. In eq. 6, the terms T_1, T_4 and D_2 are unclosed and require modelling. The term T_2 (T_3) involve the turbulent scalar flux $\overline{\rho u_j'' Y_F''}$ ($\overline{\rho u_j'' \xi''}$), which requires modelling in the context of RANS, and can be considered to be closed in the context of second-moment closure but the accuracy of evaluating these terms depends upon the modelling of $\overline{\rho u_j'' Y_F''}$ ($\overline{\rho u_j'' \xi''}$). The statistics of the unclosed terms of the $\overline{\rho Y_F'' \xi''}/\overline{\rho}$ transport equation will be discussed later in this paper.

In this work, three-dimensional DNS of statistically planar, freely-propagating turbulent stratified flames have been carried out with global ϕ values of $<\phi>=0.7$ and $<\phi>=1.0$ under decaying turbulence. The flame is initialised by an unstrained planar laminar premixed flame solution for equivalence ratio ϕ. A random bi-modal distribution of ϕ is introduced in the unburned reactants using a pseudo-spectral method [7], whereas turbulence is initialised by a homogeneous isotropic incompressible velocity field, which is generated using a standard pseudo-spectral method [8] following Batchelor-Townsend spectrum. The initial value of the rms equivalence ratio fluctuation ϕ' is 0.6 in all cases. The values of normalised initial rms turbulent velocity fluctuation $u'/S_{b(\phi=1.0)}$, integral length scale of turbulent velocity field to flame thickness ratio $l.S_{b(\phi=1.0)}/D_0$ and the ratio of integral length scale of mixture inhomogeneity to integral length scale of turbulent velocity field l_ϕ/l are listed in Table 1 along with the value of heat release parameter $\tau = (T_{ad(\phi=1)} - T_0)/T_0$ and turbulent Reynolds number Re_t. The values of Damköhler number $Da_{(<\phi>)} = lS_{b(<\phi>)}/u'\delta_{th(<\phi>)}$ and Karlovitz number $Ka_{(<\phi>)} = [u'/S_{b(<\phi>)}]^{3/2}[l.S_{b(<\phi>)}/D_0]^{-1/2}$ are listed in Table 1 where

$\delta_{th(<\phi>)} = (T_{ad<\phi>} - T_0) / Max\left|\nabla \hat{T}\right|_L$ is the thermal flame thickness of a laminar premixed flame with equivalence ratio equal to $<\phi>$, with the subscript '*L*' denoting unstrained planar laminar premixed flame quantities. For the values of $Ka_{(<\phi>)}$ in Table 1, the combustion situation belongs to the thin reaction zones (TRZ) regime [9]. Standard values are taken for Prandtl number $\mathrm{Pr} = 0.7$ and the ratio of specific heats $\gamma = C_P / C_V = 1.4$. The Zel'dovich number $\beta = T_{ac(\phi)}(T_{ad(\phi=1)} - T_0) / T^2_{ad(\phi=1)}$ is taken as $\beta = 6 f(\phi)$ where $f(\phi) = 1 + 8.25(\phi - 1)^2$ for $\phi \le 0.64$; $1 + 1.443(\phi - 1.07)^2$ for $\phi \ge 1.07$ and $f(\phi) = 1$ for $0.64 < \phi < 1.07$ following Tarrazo *et al.* [5]. The heat release per unit mass of fuel $H_\phi = (T_{ad(\phi)} - T_0) C_P / Y_{F0(\phi)}$ is given by: $H_\phi / H_{\phi=1} = 1$ for $\phi \le 1$ and $H_\phi / H_{\phi=1} = 1 - \alpha_H(\phi - 1)$ for $\phi > 1$ where α_H is given by $\alpha_H = 0.21$ [5].

Table 1: Simulation parameters corresponding to the DNS database.

Case	$u' / S_{b(\phi=1)}$	$l.S_{b(\phi=1)} / D_0$	τ	Re_t	$Da_{(<\phi>)}$	$Ka_{(<\phi>)}$	$<\phi>$	ϕ'	l_ϕ / l
A	8.0	4.2	3.0	57	0.25	10	1.0	0.6	2.2
B	4.0	4.2	3.0	28.5	0.51	4	1.0	0.6	2.2
C	8.0	4.2	3.0	57	0.05	50	0.7	0.6	2.2
D	4.0	4.2	3.0	28.5	0.10	18	0.7	0.6	2.2

The simulation domain is a cube of size $28 l_f \times 28 l_f \times 28 l_f$, where l_f is the Zel'dovich thickness (i.e. $l_f = D_0 / S_{b(\phi=1.0)}$). Cartesian grid of size $200 \times 200 \times 200$ with uniform grid spacing in all three directions is used to discretise the domain. To resolve the flame structure, approximately 10 grid points are kept within $\delta_{th(\phi=1)} = 2D_0 / S_{b(\phi=1)}$. The boundaries in the direction of mean flame propagation (i.e. x_1-direction) are considered to be partially non-reflecting and are specified using the Navier-Stokes Characteristic Boundary Conditions technique and transverse directions are periodic. A 10^{th} order central difference scheme is used for spatial differentiation for the internal grid points and the order of numerical differentiation decreases to an one-sided 2^{nd} order scheme near non-periodic boundaries. A low storage third-order Runge-Kutta scheme has been used for time advancement. All the cases are run for about 2.5 initial eddy turn-over times ($t = 2.5 l / u' = 2.5 t_f$) which is greater than or comparable to the chemical time scale $D_0 / [S^2_{b(<\phi>)}(1 + \rho_0 / \rho_{b(<\phi>)})]$. At the time the statistics were extracted, both the global turbulent kinetic energy and burning rate were not changing rapidly with time. Moreover, the qualitative nature of the results presented in the paper did not change since $t = 1.5 t_f$. The temporal evolutions of global turbulent kinetic energy and burning rate were presented elsewhere [4] and are not repeated here for the sake of brevity. When statistics were extracted, the global u' decreased by 43%, 40%, 39% and 29% in cases A-D respectively, and the normalised turbulent flame speed $S_T / S_{b(<\phi>)}$ settled to 2.2, 1.7, 1.8 and 1.5 for cases A-D respectively, where S_T is defined by $S_T = -\int \dot{\omega}_F d\vartheta / \rho_0 A_P <Y_{F0}>$ where $<Y_{F0}>$ is the mean fuel mass fraction in the unburned gas ahead of the flame, A_P is the projected flame area in the direction of the flame propagation, and $d\vartheta$ is an infinitesimal volume element. The Reynolds/Favre averaged values of the relevant quantities are evaluated

by ensemble averaging over a number of planes normal to the direction of mean flame propagation [4]. The statistical convergence of the Reynolds/Favre averaged quantities are assessed by comparing the values based on half of the samples in the transverse direction with the corresponding quantities evaluated based on full sample size. The agreement between the Reynolds/Favre averaged values based on half and full sample size are found to be satisfactory. In this paper, for the sake of brevity, only the results obtained based on full sample size will be presented.

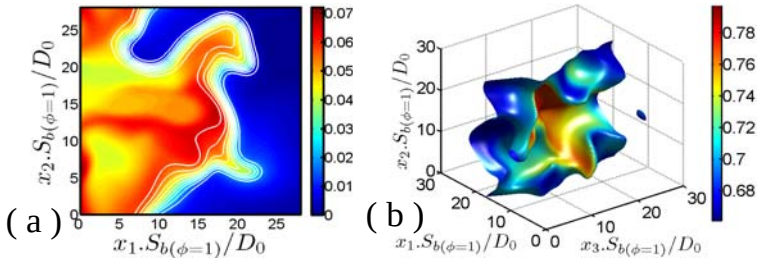

Figure 1 (a) The Y_F field at the central $x_1 - x_2$ plane at $t = 2.5t_f$ for case A. The white lines indicate the contours of c from $0.1 - 0.9$ from left to right in steps of 0.1. (b) The $c = 0.8$ iso-surface coloured with local ϕ at $t = 2.5t_f$ for case C.

Results and Discussion

Figure 1a shows the Y_F field at the central $x_1 - x_2$ plane at $t = 2.5t_f$ for case A, where the white lines indicate the c contours from 0.1 to 0.9 from left to right in steps of 0.1. Figure 1a shows that c contours representing the preheat zone (i.e. $c \le 0.5$) are more distorted than those representing the reaction zone (i.e. $0.7 \le c \le 0.9$), which is typical of the TRZ regime combustion where the flame thickness (Kolmogorov length scale η) remains greater than the Kolmogorov length scale η (reaction zone thickness). As a result of this, energetic turbulent eddies penetrate into the flame and distort the preheat zone whereas the reaction zone retains its quasi-laminar structure. It can be seen from Fig. 1a that Y_F varies in the unburned reactants and does not remain constant across a given c iso-surface, which is also substantiated by Fig. 1b where $c = 0.8$ iso-surface is coloured with local values of ϕ.

As cases A-D are statistically planar in nature, $\widetilde{c}$ remains a unique function of the co-ordinate in the direction of mean flame propagation (i.e. x_1-direction) and thus, the variations of all the terms relevant to $\overline{\rho Y_F'' \xi''} / \overline{\rho}$ transport will henceforth be presented as a function of $\widetilde{c}$. Figures 2a-d demonstrate that the model given by eq. 5 predicts the general qualitative trend of $\overline{\rho Y_F'' \xi''} / \overline{\rho}$ but over-predicts its magnitude for $< \phi >= 0.7$ cases, but eq. 5 significantly under-predicts the magnitude of $\overline{\rho Y_F'' \xi''} / \overline{\rho}$ in the reaction zone for $< \phi >= 1.0$ cases (cases A and B). Moreover, eq. 5 does not capture the behaviour of $\overline{\rho Y_F'' \xi''} / \overline{\rho}$ in the reaction zone and this limitation is more apparent in $< \phi >= 1.0$ cases than in the $< \phi >= 0.7$ cases. It should be noted that eq. 5 is derived based on eq. 3 where $\widetilde{P}(Y_F, \xi)$ is expressed in terms of discrete delta functions [3]. As $\widetilde{P}(Y_F, \xi)$ cannot be approximated by eq. 3 for low Da combustion [4], the expression for $\overline{\rho Y_F'' \xi''} / \overline{\rho}$, which is derived based on eq. 3, also becomes invalid for small values of Da. Ribert *et al.* [2] modelled $\overline{\rho Y_F'' \xi''} / \overline{\rho}$ as a function of

$\overline{\rho Y_F''^2}/\overline{\rho}$ and $\overline{\rho \xi''^2}/\overline{\rho}$ (i.e. $\overline{\rho Y_F'' \xi''}/\overline{\rho} = (\overline{\rho Y_F''^2}/\overline{\rho})^{1/2} \times (\overline{\rho \xi''^2}/\overline{\rho})^{1/2}$). The variations of $(\overline{\rho Y_F''^2}/\overline{\rho})^{1/2} \times (\overline{\rho \xi''^2}/\overline{\rho})^{1/2}$ are compared with $\overline{\rho Y_F'' \xi''}/\overline{\rho}$ variation obtained from DNS in Figs. 2a-d. Figures 2a and b show that $(\overline{\rho Y_F''^2}/\overline{\rho})^{1/2} \times (\overline{\rho \xi''^2}/\overline{\rho})^{1/2}$ significantly over-predicts the magnitude of $\overline{\rho Y_F'' \xi''}/\overline{\rho}$ and does not even capture the qualitative behaviour of $\overline{\rho Y_F'' \xi''}/\overline{\rho}$ in $<\phi>=1.0$ cases. By contrast, the qualitative behaviour of $\overline{\rho Y_F'' \xi''}/\overline{\rho}$ can be predicted by $(\overline{\rho Y_F''^2}/\overline{\rho})^{1/2} \times (\overline{\rho \xi''^2}/\overline{\rho})^{1/2}$ for $<\phi>=0.7$ cases (see Figs. 4c and d) but $(\overline{\rho Y_F''^2}/\overline{\rho})^{1/2} \times (\overline{\rho \xi''^2}/\overline{\rho})^{1/2}$ significantly over-predicts the magnitude of $\overline{\rho Y_F'' \xi''}/\overline{\rho}$. The above findings suggest that algebraic expressions may not be sufficient to capture $\overline{\rho Y_F'' \xi''}/\overline{\rho}$ behaviour for small values of Da and it may be necessary to solve a modelled transport equation for $\overline{\rho Y_F'' \xi''}/\overline{\rho}$.

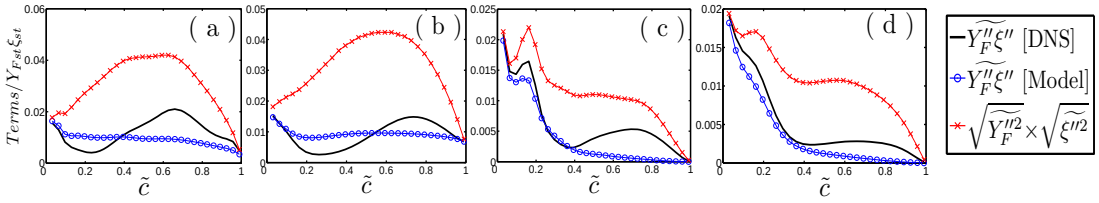

Figure 2 Variations of $\overline{\rho Y_F'' \xi''}/\overline{\rho}$ with $\tilde{c}$ across the flame-brush along with the predictions of eq. 5 and $(\overline{\rho Y_F''^2}/\overline{\rho})^{1/2} \times (\overline{\rho \xi''^2}/\overline{\rho})^{1/2}$ for cases: (a) A, (b) B, (c) C and (d) D. All terms in (a)-(d) are normalised using $Y_{Fst}\xi_{st}$.

For statistically planar stratified flames the transport equation of $\overline{\rho Y_F'' \xi''}/\overline{\rho}$ (eq. 6) takes the following form:

$$\frac{\partial}{\partial t}\left(\overline{\rho}\,\widetilde{Y_F''\xi''}\right) + \frac{\partial}{\partial x_1}\left(\overline{\rho}\widetilde{u}_1\,\widetilde{Y_F''\xi''}\right) = \underbrace{\frac{\partial}{\partial x_1}\left[\rho D \frac{\partial \widetilde{Y_F''\xi''}}{\partial x_1}\right]}_{D_1} \underbrace{- \frac{\partial(\overline{\rho u_1'' Y_F'' \xi''})}{\partial x_1}}_{T_1} \underbrace{- \overline{\rho u_1'' \xi''} \frac{\partial \widetilde{Y}_F}{\partial x_1}}_{T_2} \underbrace{- \overline{\rho u_1'' Y_F''} \frac{\partial \widetilde{\xi}}{\partial x_1}}_{T_3} + \underbrace{(\overline{\dot{\omega}_F \xi} - \overline{\dot{\omega}}\widetilde{\xi})}_{T_4} \underbrace{- 2\overline{\rho}\widetilde{\varepsilon}_{Y_\xi}}_{D_2} \quad (7)$$

The variations of the terms on the right hand side of eq. 7 with $\tilde{c}$ across the flame brush are shown in Figs. 3a-d for cases A-D. Figures 3a-d indicate that T_1 remains a major contributor in all cases exhibiting large positive values towards the unburned gas side, before decreasing to smaller values for the rest of the flame-brush. The term T_2 is predominantly negative in all cases, but does exhibit some small positive values. The term T_3 shows similar behaviour in all cases exhibiting predominantly negative values towards the unburned gas side before becoming positive towards the burned gas side of the flame-brush with a transition close to the middle of the flame-brush. The contributions of T_2 and T_3 remain small in comparison to the contributions of T_1 and T_4 for all cases. The reaction rate term T_4 exhibits both positive and negative values and remains a major contributor in $<\phi>=1.0$ cases, but becomes less important in $<\phi>=0.7$ cases. The term D_1 assumes small positive values towards the unburned gas side but becomes negative towards the reaction zone before assuming positive values again towards the burned gas side of the flame-brush in $<\phi>=1.0$ cases. In $<\phi>=0.7$ cases, the transition from positive to negative values of D_1 takes place closer to

the unburned gas side than in $<\phi>=1.0$ cases. The term $-D_2$ has been found to be a major contributor in all cases and remains predominantly negative in all cases, but exhibits small positive values in the region $0.15 \le \tilde{c} \le 0.3$ in case B. It should be noted that $-D_2$ assumes non-zero values at $c \approx 0$ due to mixture inhomogeneity. As the terms T_2 and T_3 are closed in the context of second moment closure, the modelling of T_1, T_4 and D_2 will be addressed next in this paper.

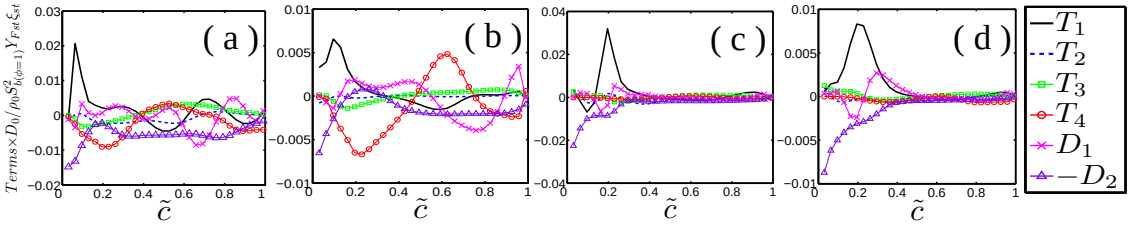

Figure 3 Variations of the terms T_1, T_2, T_3, T_4, D_1 and $-D_2$ with $\tilde{c}$ across the flame-brush for cases: (a) A, (b) B, (c) C and (d) D. All the terms are normalised with respect to $\rho_0 Y_{Fst} \xi_{st} S^2_{b(\phi=1)} / D_0$.

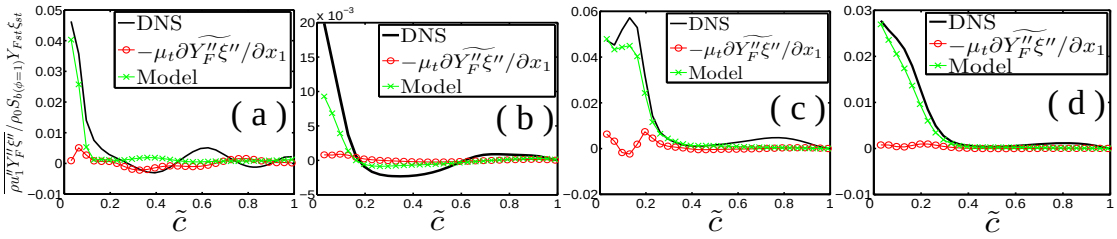

Figure 4 Variations of $\overline{\rho u_1'' Y'' \xi''} / \rho_0 S_{b(\phi=1)} Y_{Fst} \xi_{st}$ with $\tilde{c}$ across the flame-brush with the model predictions of $-\mu_t \partial(\overline{\rho Y_F'' \xi''} / \overline{\rho}) / \partial x_1$ and eq. 8 for cases: (a) A, (b) B, (c) C, (d) D.

The expression of T_1 indicates that the modelling of this term translates to the modelling of $\overline{\rho u_1'' Y_F'' \xi''}$. The variations of $\overline{\rho u_1'' Y_F'' \xi''}$ with $\tilde{c}$ for cases A-D are shown in Figs. 4a-d respectively, which demonstrate that $\overline{\rho u_1'' Y_F'' \xi''}$ assumes positive values towards the unburned gas side of the flame-brush, before assuming small values towards the burned gas side for all cases. In $<\phi>=1.0$ cases, small negative values of $\overline{\rho u_1'' Y_F'' \xi''}$ have been observed but the magnitude of the negative contribution remains small. The quantity $\overline{\rho u_1'' Y_F'' \xi''}$ is often modelled using the gradient hypothesis $\overline{\rho u_1'' Y_F'' \xi''} = -\mu_t \partial(\overline{\rho Y_F'' \xi''} / \overline{\rho}) / \partial x_1$ [2] where $\mu_t = 0.09 \overline{\rho} \tilde{k}^2 / \tilde{\varepsilon}$ is the eddy viscosity, σ is a turbulent Schmidt number, $\tilde{k} = \overline{\rho u_i'' u''} / 2\overline{\rho}$ is the turbulent kinetic energy and $\tilde{\varepsilon} = \overline{\mu \partial u_i'' / \partial x_j \cdot \partial u_i'' / \partial x_j} / \overline{\rho}$ is its dissipation rate. Figures 4a-d show that $-\mu_t \partial(\overline{\rho Y_F'' \xi''} / \overline{\rho}) / \partial x_1$ cannot accurately predict the qualitative behaviour of $\overline{\rho u_1'' Y_F'' \xi''}$ and it has been found that σ needs to be modified from one case to another for capturing the correct magnitude of $\overline{\rho u_1'' Y_F'' \xi''}$, as obtained from DNS data. An expression for $\overline{\rho u_1'' Y_F'' \xi''}$ can be derived using eq. 3 and the identity $\overline{\rho u_1'' Y_F'' \xi''} / \overline{\rho} = \int\int\int (u_1 - \tilde{u}_1)(Y_F - \tilde{Y}_F)(\xi - \tilde{\xi}) \tilde{P}(u_1, Y_F, \xi) du_1 dY_F d\xi$ as follows:

$$\widetilde{u_1''Y_F''\xi''} = \lambda_W \widetilde{u_1''\xi''^2} + (1-\lambda_W)\widetilde{A}\widetilde{u_1''\xi''^2} + [(\widetilde{u_1''Y_F''} - \lambda_W \widetilde{u_1''\xi''} - (1-\lambda_W)\widetilde{A}\widetilde{u_1''\xi''})/(\widetilde{Y}_{\max} - \widetilde{Y}_{\min})](\widetilde{\xi''^2} - \widetilde{A}\widetilde{\xi''^2}) \quad (8)$$

It is evident from Figs. 4a-d that eq. 8 captures the qualitative behaviour of $\overline{\rho u_1''Y_F''\xi''}$ satisfactorily for all cases. Although eq. 8 is derived based on eq. 3, which is strictly valid for high *Da* flames, the quantitative agreement between the prediction of eq. 8 and DNS data remains satisfactory for all the cases apart from the under-prediction towards the unburned gas side of the flame-brush in case B.

Libby and Williams [10] assumed the following presumed joint pdf $\widetilde{P}(Y_F,\xi) = \alpha_W \delta(\xi-\xi_1)\delta(Y_F - Y_{F1}) + (1-\alpha_W)\delta(\xi-\xi_2)\delta(Y_F - Y_{F2})$ where ξ_1, ξ_2, Y_{F1} and Y_{F2} are given as:

$$\xi_1 = \tilde{\xi} - (k_1\overline{\rho\xi''^2}/\bar{\rho})^{1/2},\ \xi_2 = \tilde{\xi} + (k_2\overline{\rho\xi''^2}/\bar{\rho})^{1/2},\ Y_{F1} = \tilde{Y}_F - (k_1\overline{\rho Y_F''^2}/\bar{\rho})^{1/2},\ Y_{F2} = \tilde{Y}_F + (k_2\overline{\rho Y_F''^2}/\bar{\rho})^{1/2} \quad (9a)$$

where α_W is given by: $\alpha_W = 1/(1+k_1/k_2)^{1/2}$ with $k_1 = -g_{\min}/g_{\max}$ and $k_2 = -g_{\max}/g_{\min}$ in which $g_{\max}$ and $g_{\min}$ are the maximum and minimum values of attained by a curvilinear co-ordinate g in the region bound by the equilibrium and the mixing lines on the Burke-Schumann diagram [2,3,10]. The quantity g is defined as [2,3,10]:

$$\widetilde{(\xi - \tilde{\xi})/\xi''^2} = -\widetilde{(Y_F - \tilde{Y}_F)/Y_F''^2} = \widetilde{g/g''^2} \text{ with } \tilde{g} = 0 \text{ and } \widetilde{g''^2} = \widetilde{Y_F''^2} + \widetilde{\xi''^2} \quad (9b)$$

Using $\widetilde{P}(Y_F,\xi) = \alpha_W \delta(\xi-\xi_1)\delta(Y_F - Y_{F1}) + (1-\alpha_W)\delta(\xi-\xi_2)\delta(Y_F - Y_{F2})$ one obtains:

$$\bar{\dot{\omega}}_F = \alpha_W \dot{\omega}_1 + (1-\alpha_W).\dot{\omega}_2;\ T_4 = \alpha_W \dot{\omega}_1\xi_1 + (1-\alpha_W)\dot{\omega}_2\xi_2 - [\alpha_W\dot{\omega}_1 + (1-\alpha_W)\dot{\omega}_2]\tilde{\xi} \quad (9c)$$

where $\dot{\omega}_1$ ($\dot{\omega}_2$) is the fuel reaction rate when the fuel mass fraction and mixture fraction values are given by Y_{F1} and ξ_1 (Y_{F2} and ξ_2) respectively. Robin *et al*. [3] extended this approach by considering the following $\tilde{P}(Y_F,\xi)$:

$$\widetilde{P}(Y_F,\xi) = \alpha_4\widetilde{P}_1(Y_F)\delta(\xi-\xi_{41}) + (1-\alpha_4)\widetilde{P}_2(Y_F)\delta(\xi-\xi_{42}) \quad (10a)$$

where $\widetilde{P}_1(Y_F)$ and $\widetilde{P}_2(Y_F)$ are given by [3]:

$$\widetilde{P}_1(Y_F) = \beta_4\delta(Y_F - Y_{F11}) + (1-\beta_4)\delta(Y_F - Y_{F12});\ \widetilde{P}_2(Y_F) = \gamma_4\delta(Y_F - Y_{F21}) + (1-\gamma_4)\delta(Y_F - Y_{F22}) \quad (10b)$$

In eqs. 10a and 10b the coefficients α_4, β_4 and γ_4 are expressed as [3]:

$$\alpha_4 = (\xi^{\max} - \tilde{\xi})/(\xi^{\max} - \xi^{\min});\ \beta_4 = (Y_{F1}^{\max} - \tilde{Y}_{F1})/(Y_{F1}^{\max} - Y_{F1}^{\min});\ \gamma_4 = (Y_{F2}^{\max} - \tilde{Y}_{F2})/(Y_{F2}^{\max} - Y_{F2}^{\min}) \quad (10c)$$

According to Robin *et al.* [3] the quantities $\xi_{41}, \xi_{42}, Y_{F1}$ and Y_{F2} are given by:

$$\xi_{41} = \tilde{\xi} - [((1-\alpha_4)/\alpha_4)(\overline{\rho\xi''^2}/\rho)]^{1/2};\ \xi_{42} = \tilde{\xi} + [(\alpha_4/(1-\alpha_4))(\overline{\rho\xi''^2}/\rho)]^{1/2};$$
$$Y_{F1} = \tilde{Y}_F - [((1-\alpha_4)/\alpha_4)(\overline{\rho Y_F''^2}/\bar{\rho})]^{1/2};\ Y_{F2} = \tilde{Y}_F + [(\alpha_4/(1-\alpha_4))(\overline{\rho Y_F''^2}/\bar{\rho})]^{1/2} \quad (10d)$$

In eq. 10b, the quantities $Y_{F11}, Y_{F12}, Y_{F21}$ and Y_{F22} are given by [3]:

$$Y_{F11} = \tilde{Y}_{F1} - [((1-\beta_4)/\beta_4)(\overline{\rho Y_{F1}''^2}/\bar{\rho})]^{1/2};\ Y_{F12} = \tilde{Y}_{F1} - [(\beta_4/(1-\beta_4))(\overline{\rho Y_{F1}''^2}/\bar{\rho})]^{1/2};$$
$$Y_{F21} = \tilde{Y}_{F2} - [((1-\gamma_4)/\gamma_4)(\overline{\rho Y_{F2}''^2}/\bar{\rho})]^{1/2};\ Y_{F22} = \tilde{Y}_{F2} - [(\gamma_4/(1-\gamma_4))(\overline{\rho Y_{F2}''^2}/\bar{\rho})]^{1/2} \quad (10e)$$

The quantities $\xi^{\max}$ and $\xi^{\min}$ are maximum and minimum values of ξ within the domain of definition and $Y_{F1}^{\max}$ and $Y_{F1}^{\min}$ ($Y_{F2}^{\max}$ and $Y_{F2}^{\min}$) are the maximum and minimum values of fuel mass fraction at ξ_{41} (ξ_{42}) [3]. The variances $(\overline{\rho Y_{F1}''^2}/\bar{\rho})$ and $(\overline{\rho Y_{F2}''^2}/\bar{\rho})$ are evaluated as [3]:

$$\widetilde{Y_F''^2}+\widetilde{Y}_F^{\,2}=\alpha_4(\widetilde{Y_{F1}''^2}+\widetilde{Y}_{F1}^{\,2})+(1-\alpha_4)(\widetilde{Y_{F2}''^2}+\widetilde{Y}_{F2}^{\,2}),\ \widetilde{Y_{F1}''^2}/\widetilde{Y_{F2}''^2}=(Y_{F1}^{\max}-\widetilde{Y}_{F1})(\widetilde{Y}_{F1}-Y_{F1}^{\min})/[(Y_{F2}^{\max}-\widetilde{Y}_{F2})(\widetilde{Y}_{F2}-Y_{F2}^{\min})] \quad (10f)$$

According to eq. 10a the quantities $\overline{\dot{\omega}}_F$ and T_4 are modelled as [3]:

$$\overline{\dot{\omega}}_F = \alpha_4\beta_4\dot{\omega}_A + \alpha_4(1-\beta_4)\dot{\omega}_B + (1-\alpha_4)\gamma_4\dot{\omega}_C + (1-\alpha_4)(1-\gamma_4)\dot{\omega}_D \quad (10g)$$

$$\begin{aligned} T_4 = {} & \alpha_4\beta_4\dot{\omega}_A\xi_{41} + \alpha_4(1-\beta_4)\dot{\omega}_B\xi_{42} + (1-\alpha_4)\gamma_4\dot{\omega}_C\xi_{41} + (1-\alpha_4)(1-\gamma_4)\dot{\omega}_D\xi_{42} \\ & -[\alpha_4\beta_4\dot{\omega}_A + \alpha_4(1-\beta_4)\dot{\omega}_2 + (1-\alpha_4)\gamma_4\dot{\omega}_C + (1-\alpha_4)(1-\gamma_4)\dot{\omega}_D]\widetilde{\xi} \end{aligned} \quad (10h)$$

where $\dot{\omega}_A$ and $\dot{\omega}_B$ ($\dot{\omega}_C$ and $\dot{\omega}_D$) are the fuel reaction rates when the fuel mass fraction values are given by Y_{F11} and Y_{F12} (Y_{F21} and Y_{F22}) respectively at a mixture fraction ξ_{41} (ξ_{42}). The predictions of eqs. 9c and 10h are shown in Figs. 5a-d for cases A-D respectively. Figures 5a-d show that both the models given by eqs. 9c and 10h over-predict the magnitude of T_4 in all cases. However, the prediction of eq. 9c remains predominantly positive throughout the flame-brush, but eq. 10h exhibits negative values towards the burned gas side. It should be noted that whilst deriving the models given by eqs. 9c and 10h, $\widetilde{P}(Y_F,\xi)$ was approximated by discrete delta functions [3]. However, a recent analysis [3] demonstrated that $\widetilde{P}(Y_F,\xi)$ cannot be approximated in terms of discrete delta functions for low *Da* combustion. The extent of the inaccuracy incurred by approximating $\widetilde{P}(Y_F,\xi)$ by discrete delta functions can be characterised in terms of segregation factor S which can be defined as [3]:

$$S=\left(\widetilde{Y_F''^2}-\{(\widetilde{Y}_F-\widetilde{Y}_{\min})/(\widetilde{Y}_{\max}-\widetilde{Y}_{\min})+(\widetilde{Y}_{\max}-\widetilde{Y}_F)/(\widetilde{Y}_{\max}-\widetilde{Y}_{\min})\widetilde{A}^2\}\widetilde{\xi''^2}\right)\times((\widetilde{Y}_{\max}-\widetilde{Y}_F)(\widetilde{Y}_F-\widetilde{Y}_{\min}))^{-1} \quad (11)$$

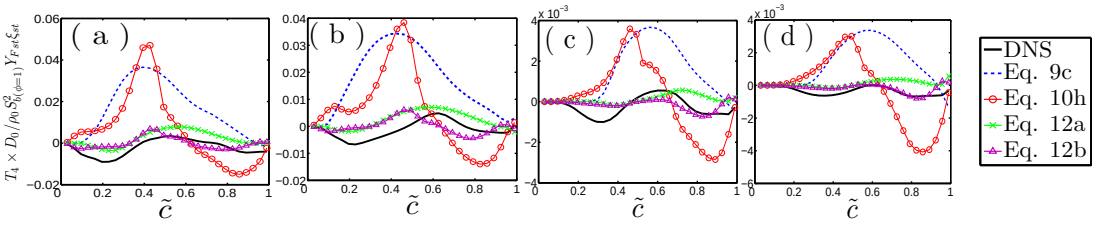

Figure 5 Variations of $T_4 \times D_0 / \rho_0 Y_{Fst}\xi_{st}S_{b(\phi=1)}^2$ with $\tilde{c}$ across the flame-brush with the prediction of the models given by eqs. 9c, 10h, 12a, 12b for cases: (a) A, (b) B, (c) C, (d) D.

For high values of *Da*, the segregation factor becomes unity (i.e. $S=1.0$) which indicates that $\widetilde{P}(Y_F,\xi)$ can be approximated by discrete delta functions [1,2,10]. For low *Da* combustion, the models given by eqs. 9c and 10h are modified as:

$$T_4 = C_S[\alpha_W\dot{\omega}_1\xi_1 + (1-\alpha_W)\dot{\omega}_2\xi_2 - [\alpha_W\dot{\omega}_1 + (1-\alpha_W)\dot{\omega}_2]\widetilde{\xi}] \quad (12a)$$

$$\begin{aligned} T_4 = C_S\{ & \alpha_4\beta_4\dot{\omega}_A\xi_{41} + \alpha_4(1-\beta_4)\dot{\omega}_B\xi_{42} + (1-\alpha_4)\gamma_4\dot{\omega}_C\xi_{41} + (1-\alpha_4)(1-\gamma_4)\dot{\omega}_D\xi_{42} \\ & -[\alpha_4\beta_4\dot{\omega}_A + \alpha_4(1-\beta_4)\dot{\omega}_2 + (1-\alpha_4)\gamma_4\dot{\omega}_C + (1-\alpha_4)(1-\gamma_4)\dot{\omega}_D]\widetilde{\xi}\} \end{aligned} \quad (12b)$$

where C_S in eqs. 12a and 12b is taken to be:

$$C_S = \{S - 0.5[(\widetilde{\xi}(1-\xi_{st}))/(\xi_{st}(1-\widetilde{\xi}))]\}/\{1-0.5[(\widetilde{\xi}(1-\xi_{st}))/(\xi_{st}(1-\widetilde{\xi}))]\} \quad (12c)$$

For large values of Da, the segregation factor S approaches to unity, giving $C_S \approx 1.0$. Therefore, eqs. 12a and 12b become equal to eqs. 9c and 10h respectively, for high values of Da. Figures 5a-d show that eqs. 12a and 12b are in better agreement with T_4 obtained from DNS data than eqs. 9c and 10h. Equation 12b captures both the qualitative and quantitative behaviour of T_4 for all cases better than the models given by eqs. 9c, 10h and 12a.

Equation 6 indicates that the modelling of D_2 is dependent upon the accurate evaluation of $\widetilde{\varepsilon}_{Y\xi}$. Mura *et al.* [3] proposed a model for $\widetilde{\varepsilon}_{Y\xi}$ as:

$$\widetilde{\varepsilon}_{Y\xi} = S\left(-\overline{\rho D}\frac{\partial \widetilde{Y}_F}{\partial x_k}\frac{\partial \widetilde{\xi}}{\partial x_k} + \frac{[\overline{\dot{\omega}_F \xi} - \overline{\dot{\omega}}_F \widetilde{\xi}]}{2}\right)\frac{1}{\overline{\rho}} + S\left(\frac{\widetilde{Y}_F - \widetilde{Y}_{\min}}{\widetilde{Y}_{\max} - \widetilde{Y}_{\min}} + \frac{\widetilde{Y}_{\max} - \widetilde{Y}_F}{\widetilde{Y}_{\max} - \widetilde{Y}_{\min}}\widetilde{A}\right) \times \widetilde{\varepsilon}_{\xi} + (1-S)C_{Y\xi}\frac{\widetilde{\varepsilon}}{\widetilde{k}}\widetilde{Y_F''\xi''} \quad (13)$$

where $C_{Y\xi}$ is a model parameter. It should be noted that the quantity $[\overline{\dot{\omega}_F \xi} - \overline{\dot{\omega}}_F \widetilde{\xi}]$ in eq. 13 is unclosed, and its modelling was addressed earlier in the context of T_4 modelling. The model given by eq. 13 will henceforth be referred to as CDM. The variations of $\widetilde{\varepsilon}_{Y\xi}$ with $\widetilde{c}$ are shown in Figs. 6a-d for cases A-D. Figures 6a-d show that $\widetilde{\varepsilon}_{Y\xi}$ assumes non-zero values at $\widetilde{c} \approx 0$ due to the mixture inhomogeneity ahead of the flame, and approaches to a negligible value at $\widetilde{c} = 1.0$ due to the smaller magnitude of fuel mass fraction gradient in the burned gas. The predictions of the model given by eq. 13 are shown in Figs. 6a-d for optimum values of $C_{Y\xi}$ evaluated using $\int_{\widetilde{c}=0.005}^{\widetilde{c}=0.995} Q_{DNS}.dx = \int_{\widetilde{c}=0.005}^{\widetilde{c}=0.995} Q_{Model}.dx$ [4,11] where subscripts DNS and Model are used to refer to quantities obtained from DNS and from the model prediction respectively. The model given by eq. 13 when $\widetilde{\varepsilon}_{\xi}$ and $[\overline{\dot{\omega}_F \xi} - \overline{\dot{\omega}}_F \widetilde{\xi}]$ are extracted from DNS data captures the qualitative and quantitative behaviours of $\widetilde{\varepsilon}_{Y\xi}$ obtained from DNS data in $<\phi>= 0.7$ cases. However, the qualitative and quantitative behaviours of $\widetilde{\varepsilon}_{Y\xi}$ are not adequately captured by eq. 13 in $<\phi>= 1.0$ cases. The CDM model significantly over-predicts $\widetilde{\varepsilon}_{Y\xi}$ at the middle of the flame-brush in cases A and B. Moreover, negative values of $\widetilde{\varepsilon}_{Y\xi}$ are predicted by eq. 13 towards the burned gas side in $<\phi>= 1.0$ cases, whereas $\widetilde{\varepsilon}_{Y\xi}$ obtained from DNS remains positive. It can further be seen from Figs. 6a-d that the optimum value of $C_{Y\xi}$ increases with increasing $u'/S_{b(\phi=1)}$ for a given value of $<\phi>$. The optimum value of $C_{Y\xi}$ is found to decrease with decreasing $<\phi>$ for $u'/S_{b(\phi=1)} = 8.0$ cases whereas a marginal increase in the optimum value of $C_{Y\xi}$ is observed when $<\phi>$ decreases from 1.0 to 0.7 for $u'/S_{b(\phi=1)} = 4.0$. However, the model given by eq. 13 does not capture the correct qualitative behaviour of $\widetilde{\varepsilon}_{Y\xi}$ even with the optimum $C_{Y\xi}$ value for $<\phi>= 1.0$ cases. For eq. 13, $\widetilde{\varepsilon}_{\xi}$ and $[\overline{\dot{\omega}_F \xi} - \overline{\dot{\omega}}_F \widetilde{\xi}]$ need to be modelled. Often $\widetilde{\varepsilon}_{\xi}$ is modelled by a linear relaxation relation $\widetilde{\varepsilon}_{\xi} = C_{\xi}(\widetilde{\varepsilon}/\widetilde{k})\overline{\rho\xi''^2}/\overline{\rho}$ where C_{ξ} is taken to be unity [3]. The prediction of the model by eq. 13 with $\widetilde{\varepsilon}_{\xi} = C_{\xi}(\widetilde{\varepsilon}/\widetilde{k})\overline{\rho\xi''^2}/\overline{\rho}$ for the optimum values of $C_{Y\xi}$ and $C_{\xi} = 1.0$ are also shown in Figs. 6a-d, where $[\overline{\dot{\omega}_F \xi} - \overline{\dot{\omega}}_F \widetilde{\xi}]$ is extracted from DNS data (denoted as CDM-LR model in the Fig. 6). Figures 6a-d suggest that, for $C_{\xi} = 1.0$, the CDM-LR model predicts greater

values than the prediction of the CDM model in $<\phi>=1.0$ cases, but the prediction of the CDM-LR model remains comparable to the values obtained from DNS in $<\phi>=0.7$ cases. This indicates the modelling of $\widetilde{\varepsilon}_{\xi}$ does affect the performance of eq. 13 for $<\phi>=1.0$ cases, but has a small affect in $<\phi>=0.7$ cases. The predictions of eq. 13, where $\widetilde{\varepsilon}_{\xi}$ is modelled as $\widetilde{\varepsilon}_{\xi}=C_{\xi}(\widetilde{\varepsilon}/\widetilde{k})\overline{\rho\xi''^{2}}/\overline{\rho}$ and $[\overline{\dot{\omega}_F\xi}-\overline{\dot{\omega}}_F\widetilde{\xi}]$ are modelled by eqs. 12a and 12b, are also shown in Figs. 6a-d, which are denoted as the CDM-2D and CDM-4D models respectively. Figures 6a-d show both the CDM-2D and CDM-4D models predict the qualitative behaviour of $\widetilde{\varepsilon}_{Y\xi}$, but they over-predict the magnitude of $\widetilde{\varepsilon}_{Y\xi}$, especially in $<\phi>=1.0$ cases. The extent of these over-predictions is small in $<\phi>=0.7$ cases where the effects of T_4 on the $\overline{\rho Y_F''\xi''}/\overline{\rho}$ transport are relatively weak. Recently, Nguyen *et al.* [12] expressed $\widetilde{\varepsilon}_{Y\xi}$ as $\widetilde{\varepsilon}_{Y\xi}=\sqrt{\widetilde{\varepsilon}_{Y}}\times\sqrt{\widetilde{\varepsilon}_{\xi}}$ but Figs. 6a-d suggest that $\sqrt{\widetilde{\varepsilon}_{Y}}\times\sqrt{\widetilde{\varepsilon}_{\xi}}$ significantly over-predicts $\widetilde{\varepsilon}_{Y\xi}$ in all cases, which is most apparent in $<\phi>=1.0$ cases, though the extent of the over-prediction reduces in $<\phi>=0.7$ cases. As the existing algebraic models are not capable of predicting the correct $\widetilde{\varepsilon}_{Y\xi}$ behaviour for all values of $<\phi>$ and $u'/S_{b(\phi=1)}$, it may be necessary to solve a modelled transport equation for $\widetilde{\varepsilon}_{Y\xi}$.

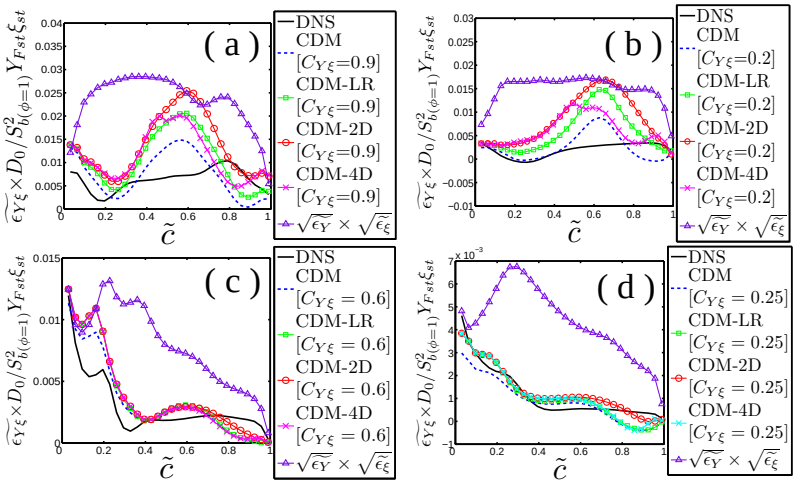

Figure 6 Variations of $\widetilde{\varepsilon}_{Y\xi}\times D_0/S^2_{b(\phi=1)}Y_{Fst}\xi_{st}$ with $\widetilde{c}$ across the flame-brush and predictions of CDM, CDM-LR, CDM-2D and CDM-4D models for cases: (a) A, (b) B, (c) C, (d) D.

Conclusions

Three-dimensional DNS of statistically planar turbulent stratified flames with $<\phi>=0.7$ and $<\phi>=1.0$ have been carried out to analyse the statistical behaviour of $\overline{\rho Y_F''\xi''}/\overline{\rho}$ transport for low *Da* combustion. The existing algebraic models do not adequately capture the behaviour of $\overline{\rho Y_F''\xi''}/\overline{\rho}$ for low *Da* combustion. The modelling and statistical behaviours of the unclosed terms of the $\overline{\rho Y_F''\xi''}/\overline{\rho}$ transport equation (i.e. T_1, T_4 and $-D_2$) have been addressed for RANS simulations. Performances of the models for the unclosed terms of the $\overline{\rho Y_F''\xi''}/\overline{\rho}$ equation have been assessed based on *a-priori* DNS analysis. A suitable model has

been identified for T_1 and suggestions have been made to improve the performances of existing models for T_4 for low *Da* combustion. Current algebraic models cannot predict cross-scalar dissipation rate $\widetilde{\varepsilon}_{Y\xi}$ for all values of $<\phi>$ and u' considered in this study. Therefore, either improved algebraic models are required to be developed, or a modelled transport equation of $\widetilde{\varepsilon}_{Y\xi}$ must be solved to obtain closure of $-D_2$. The present study has been carried out for modest values of Re_t but the arguments which were used for modelling the unclosed terms of the $\overline{\rho Y_F'' \xi''} / \overline{\rho}$ transport equation are also applicable for higher values of Re_t. The effects of detailed chemistry and differential diffusion rate of mass and heat are not considered in the present analysis. This necessitates both experimental and detailed-chemistry DNS based validation of the proposed models for higher values of Re_t.

Acknowledgements

SPM and NC gratefully acknowledge the financial assistance of the EPSRC UK.

References

[1] Ribert, G.; Champion, M.; Gicquel, O.; Darabiha, N.; Veynante, D., "Modeling nonadiabatic turbulent premixed reactive flows including tabulated chemistry". *Combust. Flame*, **141**, 271–280, (2005).

[2] Robin, V.; Mura, A.; Champion, M.; Plion, P., "A multi-Dirac presumed PDF model for turbulent reacting flows with variable equivalence ratio". *Combust. Sci. Tech.*, **178**, 1843–1870, (2006).

[3] Mura, A.; Robin, V.; Champion, M., "Modeling of scalar dissipation in partially premixed turbulent flames". *Combust. Flame*, **149**, 217-224, (2007).

[4] Malkeson, S.P.; Chakraborty, N., "A-priori Direct Numerical Simulation analysis of algebraic models of variances and scalar dissipation rates for Reynolds Averaged Navier Stokes Simulations for low Damköhler number turbulent partially-premixed combustion". *Combust. Sci. Tech.*, **182**, 960-999, (2010).

[5] Tarrazo, E.; Sanchez, A.; Linan, A.; Williams, F., "A simple one-step chemistry model for partially premixed hydrocarbon combustion". *Combust. Flame*, **147**, 32-38, (2006).

[6] Hélie, J.; Trouvé, A., "Turbulent flame propagation in partially premixed combustion". *Proc. Combust. Inst.*, **27**, 891–898, (1998).

[7] Eswaran, V.; Pope, S.B., "Direct numerical simulations of the turbulent mixing of a passive scalar". *Phys. Fluids*, **31**, 506-520, (1988).

[8] Rogallo, R.S., "Numerical experiments in homogeneous turbulence", *NASA Technical Memorandum 81315*, NASA Ames Research Center, (1981).

[9] Peters, N., Turbulent Combustion Cambridge University Press, Cambridge, UK, 2000.

[10] Libby, P.A.; Williams, F.A., "A Presumed Pdf Analysis of Partially Premixed Turbulent Combustion", *Combust. Sci. Tech..*, **161**, 351-390, (2000).

[11] Nishiki, S.; Hasegawa, T.; Borghi, R.; Himeno, R., "Modeling of flame generated turbulence using Direct Numerical Simulation databases". *Proc. Combust. Instit.*, **29**, 2017-2022, (2002).

[12] Nguyen, P.D.; Vervisch, L.; Subramanian, V.; Domingo, P., "Multidimensional flamelet-generated manifolds for partially premixed combustion". *Combust. Flame*, **157**, 43-61, (2010).